Industrial Crops & Products 248 (2026) 123473

Contents lists available at ScienceDirect

Industrial Crops & Products

journal homepage: www.elsevier.com/locate/indcrop

Mechanical and structural evolution of hemp fibre along plant maturity

Idrissa Diakite [a,*], Xavier Gabrion [b], Sylvie Durand [c], Thomas Jeannin [b], Luc Malhautier [d], Scherrine A. Tria [d], Johnny Beaugrand [c], Vincent Placet [b], Alain Bourmaud [a]

[a] Univ. Bretagne Sud, UMR CNRS 6027, IRDL, Lorient 56100, France
[b] Université Marie et Louis Pasteur, SUPMICROTECH, CNRS, institut FEMTO-ST, Besançon 25000, France
[c] UR1268 Biopolymères Interactions Assemblages, INRAE, Nantes 4316, France
[d] GARANCe, IMT Mines Ales, Ales, France

ARTICLE INFO

Keywords:
Indentation modulus
Tomography
Image analysis
AFM
Raman spectroscopy

ABSTRACT

Understanding how the structure, mechanical properties, and biochemical composition of hemp fibres evolve simultaneously is essential for optimizing their performance in textile and bio-based composite applications. In this study, hemp fibres were analysed at three developmental stages (50, 80, and 122 days after sowing) using a multi-scale approach combining optical microscopy, microtomography, nanoindentation, AFM-PF-QNM, and Raman microspectroscopy. Morphological analyses revealed progressive thickening of the cell wall and a reduction in lumen size during fibre maturation. Local measurements obtained by nanoindentation and AFM showed a significant increase in the indentation modulus, while Raman spectroscopy revealed biochemical and crystallinity changes associated with cellulose and hemicellulose. These changes are consistent with cell wall maturation and are well correlated with local stiffness variations throughout the maturation process. Beyond these global trends, heterogeneity in fibre maturation was observed. At 50 days, most fibres exhibit a large lumen, indicating an early stage of maturity. However, a fraction of fibres (3.9%) can be morphologically distinguished by a thick secondary cell wall and a reduced lumen; these are referred to here as "filled fibres." These filled fibres at 50 days display high cell wall mechanical properties, in contrast to other fibres at the same stage, and exhibit values comparable to those measured at 80 days, where 32.3% of fibres have thick walls, and at 122 days, where this proportion reaches 80.7%. Furthermore, differences in biochemical composition were observed between thick-walled and thin-walled fibres as early as 50 days, indicating that some fibres reach an advanced stage of maturation earlier than others. By combining morphological, nanomechanical, and spectroscopic analyses, this study quantifies the simultaneous evolution of cell wall properties, highlights the asynchronous nature of hemp fibre maturation, and reveals a correlation between increasing cellulose crystallinity and nanoindentation modulus, reflecting progressive cell wall structuring.

1. Introduction

Synthetic fibres are widely used across various industries due to their high mechanical performance and durability in service. However, their environmental impact raises significant concerns: they are neither biodegradable nor bio-based, their production is energy-intensive, and they may pose risks to human health (Yuan Z., et al., 2022).

In response to these challenges, bio-based materials have garnered increasing attention in both industrial and academic spheres. Among these, plant fibres stand out as sustainable alternatives to synthetic fibres for numerous applications, particularly in bio-based composites and textiles. Within plant fibres, hemp holds a special position. Indeed, it is one of the oldest known textile crops, cultivated for over 6000 years (Small, 2015). Thanks to its high mechanical strength (Duval et al., 2011; Bourmaud et al., 2018), light weight (Aziz and Ansell, 2004), and biodegradability (Islam et al., 2011; Stamboulis et al., 2001), hemp fibre is a particularly attractive material to use in composites, textiles, construction.

Nevertheless, the quality of hemp fibres is highly variable, which in turn affects their mechanical performance. This variability is influenced by several factors, including plant variety (Marrot et al., 2013), developmental stage (Mediavilla et al., 2001), growth conditions such as soil type and climate (van der Werf et al., 1995), as well as extraction, separation processes, notably retting (Müssig and Beaugrand 2025;

* Corresponding author.
E-mail address: idrissa.diakite@univ-ubs.fr (I. Diakite).

https://doi.org/10.1016/j.indcrop.2026.123473
Received 1 September 2025; Received in revised form 5 May 2026; Accepted 10 May 2026
Available online 15 June 2026

Müssig et al., 2020; Placet et al., 2017; Liu et al., 2015).

From a biological point of view, hemp fibres are long, thick-walled cells that form bundles within the stem. They can reach several tens of millimetres in length and several tens of micrometres in diameter (Gorshkova et al., 2012). Two types of phloem fibres can be present in hemp stems. Primary fibres, located in the outer phloem at the stem periphery, develop early and extend longitudinally along the stem, from the base to the apex (Hernandez et al., 2007; Snegireva et al., 2015). Secondary fibres may also appear in the basal part of mature stems, depending on the cultivar and growing conditions (Chernova et al., 2018). They provide additional mechanical support but are generally considered less suitable for high-value textile or composite applications due to their morphology (Bourmaud et al., 2017).

Hemp fibres, like flax fibres (Baley, 2002), are composed of concentric cell wall layers surrounding a central lumen. The outermost primary wall is relatively thin (0.1–0.2 μm) (Bos and Donald, 1999), while the secondary wall is thicker and consists of three layers (S1, S2, S3). The S2 layer is the most prominent, representing about 80% of the total wall thickness, and is composed of highly crystalline cellulose microfibrils embedded in a matrix of hemicelluloses and pectins (Crônier et al., 2005; Goubet et al., 1995).

Moreover the chemical composition of the cell wall strongly influences mechanical properties. Cellulose, which has the highest elastic modulus (Kroon-Batenburg et al., 1986; Salmén, 2004), is the main determinant of fibre stiffness. The balance between structural and matrix pectins also affects wall cohesion and organisation (Lefeuvre et al., 2015).

During fibre maturation, the structure and composition of cell wall change, leading to alterations in its mechanical properties (Kim et al., 2021). For example, gradual thickening of the wall has been observed in flax fibres (Goudenhooft et al., 2018), contributing to a mechanical strengthening. These structural and mechanical changes are essential for understanding fibre performance and determining the optimal harvest stage for industrial applications.

In addition, several studies have demonstrated that the tensile strength and stiffness of fibres are highly dependent on their diameter (Hu et al., 2010; Andersons et al., 2005; Zafeiropoulos and Baillie, 2007).

Traditionally, the mechanical properties of hemp fibres are evaluated through tensile testing, which provides an apparent Young's modulus measured at the scale of the entire fibre. Complementary techniques such as nanoindentation and atomic force microscopy (AFM) have been increasingly used to investigate the local mechanical properties of plant fibre cell walls. In the literature several studies have applied these methods to hemp fibres. (Marrot et al.,2013) employed nanoindentation to assess fibre mechanical properties, while (Bourmaud et al., 2017) combined nanoindentation and AFM to compare the mechanical behaviour of primary and secondary fibres. The literature generally reports a high variability in the mechanical properties of individual hemp fibres, with tensile Young's modulus values ranging from approximately 14 GPa (Placet, 2009) to more than 32 GPa (Sawpan et al., 2011, Pinsard et al., 2023) depending on the study. Similarly, indentation modulus values measured using nanoindentation or AFM typically range between 15 and 23 GPa (Marrot et al.,2013; Bourmaud et al.,2017).

This variability highlights both the diversity of the evaluation techniques used and the intrinsic heterogeneity of hemp fibres, which can vary significantly even within the same stem (Beaugrand et al., 2014).

It is also important to note that tensile testing and indentation techniques probe different mechanical scales. Tensile testing evaluates the apparent Young's modulus of the whole fibre, whereas nanoindentation and AFM probe the mechanical behaviour locally at the level of the cell wall. As a result, indentation measurements reflect the local mechanical response of the cell wall and provide insight into the structural organisation of the wall layers that cannot be captured by conventional tensile tests, the latter being strongly influenced by local defects at the fibre scale.

Despite these advances, most studies have addressed fibre morphology, biochemical composition and mechanical properties separately. Crônier et al. (2005) studied the development of the cell walls of hemp fibres at different stages of maturity focusing on changes in major structural components, including carbohydrates, phenolic compounds, and proteins. Although this study provided important insights into biochemical changes during fibre development, it did not include a direct analysis of mechanical properties during maturation. Similarly, (Kim et al.,2021) investigated structural changes in fibre cell walls as a function of developmental stage but did not link these observations to local mechanical characterization or detailed biochemical analysis.

Consequently, the quantitative relationships between fibre morphology, biochemical organisation of the cell wall, and the local mechanical properties during fibre maturation remain poorly documented.

In this context, the present study aims to investigate the structural and mechanical evolution of hemp fibre cell walls during maturation by combining several complementary experimental techniques. Optical microscopy and X-ray microtomography are used to quantify fibre morphology, particularly lumen size and cell wall thickness. Micro-Raman spectroscopy is employed to monitor changes in biochemical composition during fibre maturation. Finally, nanoindentation and atomic force microscopy operating in PeakForce QNM mode provide high-resolution mapping of local stiffness within the fibre wall. This integrated approach makes it possible to establish correlations between fibre morphology, biochemical organisation, and mechanical behaviour during maturation.

2. Materials and methods

2.1. Plant material

Hemp (Cannabis sativa, variety Santhica 70) was grown under field conditions on April 29, 2024, in Piégros-la-Clastre (Drôme, southern France). Hemp was cultivated on alluvial soil with a relatively high clay content. Stems were harvested at three developmental stages: June 18 (T1, 50 days after sowing), July 18 (T2, 80 days after sowing), and August 29 (T3, 122 days after sowing), the latter corresponding to the final harvest prior to retting. The sowing density was 70–80 $kg{\cdot}ha^{-1}$. No fertilizer was applied, and the field was not irrigated during plant growth. T1 and T2 correspond to the active growth phase, extending from plant emergence to the onset of flowering. The final harvest (T3) was performed at the end of the flowering stage. In this study, fibre analyses were performed in planta on samples collected from the middle section of the stem.

It is important to note that fibre properties may vary significantly along the stem height due to asynchronous development. Therefore, the present results may differ from literature data obtained from other stem regions. All comparisons across the three developmental stages were conducted on samples taken from the same median region of the stem, ensuring consistency in the assessment of maturation trends.

Meteorological data, including daily minimum and maximum temperatures and rainfall, were obtained from local monitoring (Météo-France). As shown in Fig. 1, weather conditions varied considerably throughout the growing season, with a progressive increase in temperature, reaching up to 38 °C during summer, and heterogeneous rainfall. A pronounced dry period occurred in July and August, with only eight rainy days over these two months, corresponding to 46 mm (approximately 12.5% of the total rainfall from sowing to T3 sampling). Immediately after collection, the samples were preserved in an ethanol/water solution (70/30, v/v) for subsequent analysis.

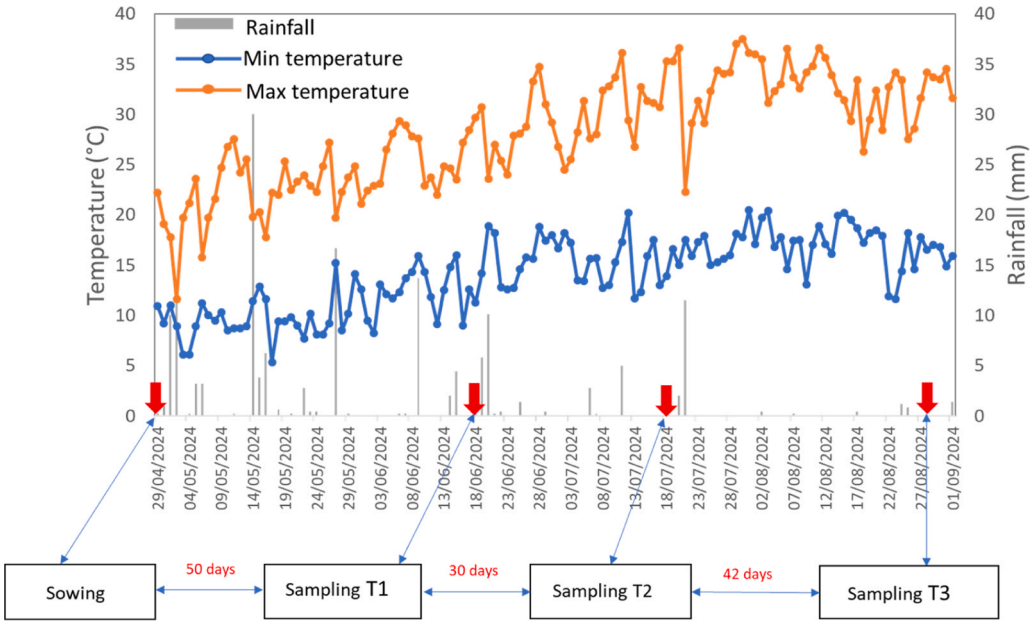

Fig. 1. Daily minimum and maximum temperatures, and rainfall during plant growth.

2.2. Sample preparation for microscopic investigations

Stem segments less than 1 cm in length were cut and progressively dehydrated. The samples were first immersed in 100% ethanol for 1 h at room temperature, before being transferred to 100% acetone for 30 min. This step ensures optimal transition for resin impregnation (https://myscope.training/).

Embedding in resin was performed in two stages. First, fibres were gradually impregnated in a mixture of low-viscosity Agar resin and acetone (50/50v/v) for 1 h, followed by final immersion in 100% resin for 1 h. Final polymerization was carried out in an oven (Heraeus Thermo Scientific) at 60°C overnight. Once polymerized, the resin blocks were cut using a diamond wire saw (well, model 3500) to obtain 3–4 mm fragments. These fragments were then glued onto circular metal supports.

Surface preparation for specimen analysis was carried out using an ultramicrotome (Leica Ultracut R, Wetzlar, germany) equipped with diamond knives (Trim Diatome and Ultra AFM, Nidau, Switzerland). A reduced cutting speed (≈1 mm/s) was applied to minimize topographic artifacts and ensure an optimal surface for nanomechanical measurements.

Sample preparation is a critical step in this study. It is well established that dehydration procedures prior to embedding, as well as the embedding medium itself, can alter the mechanical properties of the cell wall (Meng et al., 2012). These effects may introduce potential biases in nanomechanical measurements. Such biases can be stage-dependent. Young fibres, characterized by thinner and more porous walls, are likely to experience greater infiltration of the embedding medium than mature fibres, which can lead to apparent differences in mechanical properties between developmental stages.

However, the use of an embedding medium is necessary to preserve the structural integrity of the cell wall during subsequent surface preparation. In particular, embedding prevents mechanical damage and detachment of the G-layer (Clair et al., 2005). Moreover, embedding improves sample stability and reduces surface roughness artefacts and edge effects, which is essential for obtaining reliable Peak Force QNM AFM measurements (Arnould and Arinero, 2015).

2.3. Morphological analysis

The morphological evolution of hemp fibres was studied using a Keyence VHX-S770E optical microscope, based on stem cross-sections prepared as described above. Detailed observations were performed to characterise structural variations in stem sections at different stages of maturity. Additionally, X-ray tomography (RX Solution) was carried out on the same sample prior to resin impregnation to provide complementary morphological information. The stems were cut into quarters to improve imaging resolution, with approximate dimensions of $2 \times 1 \times 10$ mm^3. The samples were placed in Eppendorf microtubes (0.5 ML) to preserve moisture content. The samples were placed on the rotating stage of the machine. Acquisition parameters included a tube voltage of 60 keV and a current of 122 µA. A total of 1440 projections were taken in four turns (each 0.25°) with an exposure time of 1000 ms and an average of 2 images, resulting in a total scan time of approximately 60 min. The voxel size was fixed at 1.2 µm, and reconstructions were performed using filtered back projection implemented in Xact software (RX Solution). The 3D renderings and segmentation were produced using VG StudioMax 2025.1 software (Fig. 2).

In addition to 3D visualization, a morphological analysis of the binary images was performed to quantitatively assess the internal structure of the fibres. This analysis was conducted using a custom MATLAB script. The binary images were first manually thresholded to remove noise by excluding the smallest particles (artifacts) and the largest ones (likely resulting from cell fusion). Once a clean segmentation was obtained, the centroids of individual fibres were detected. For each fiber, the area of each lumen was determined by counting the number of pixels and converting the scale.

Feret diameters were then computed to determine both the minimum and maximum diameters of the elliptical lumens, providing insight into fibre shape variability. The Feret diameter corresponds to the distance between two parallel tangents on opposite sides of the fibre boundary, measured at a given orientation. This measurement reflects the distance between two opposing points of the object projected in a specific direction, offering a robust estimate of the "apparent diameter" of the fiber cross-section. The maximum Feret diameter is obtained by identifying the largest distance between two opposing points of the object across all orientations, whereas the minimum Feret diameter corresponds to the smallest such distance. This approach is particularly well suited for

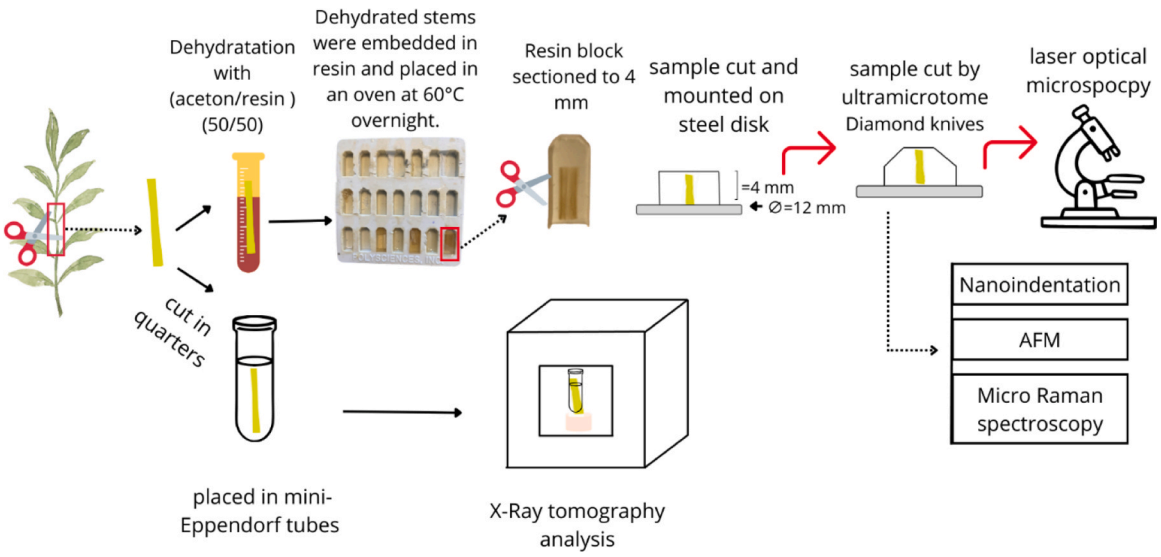

Fig. 2. Schematic of hemp stems sample preparation for multi-scale analyses.

characterizing non-circular fibres, as it captures variations in shape and orientation, unlike methods based on an assumed equivalent circular diameter.

Once the wall thickness values were determined, an external contour line representing the outer surface of the stem section was manually or semi-automatically traced. Each fibre was then spatially located with respect to this external boundary. This enabled us to analyse how fibre wall thickness varies according to their radial position within the stem, particularly in relation to their proximity to the epidermis. This spatial mapping provided valuable insight into the maturation gradient and structural organisation of the fibre bundle across the stem cross-section. To assess the robustness of the custom MATLAB detection algorithm, multiple images were extracted along the height (each 50 μm on 500μm) of the hemp stem to evaluate the consistency of the results. These cross-sections showed good reproducibility in fibre detection and morphological

quantification, indicating reliable performance of the image processing pipeline. Additionally, to validate the automation of the image processing procedure, a subset of 10 fibres was manually measured for minimum and maximum Feret diameters as well as wall thickness. The comparison showed very small discrepancies, below 3 pixels for minimum Feret diameters, 2 pixels for maximum Feret diameters, and 1 pixel for wall thickness measurements. Based on this validation, a single representative image was selected for each maturity level. This approach allowed for the analysis of approximately one hundred fibres per condition, ensuring statistically meaningful and reproducible results across all stages of plant development.

2.4. Nanoindentation (NI) measurements

Nanoindentation analyses were carried out using a commercial Nanoindenter XP system (MTS Nano Instruments), under controlled conditions of 23°C and 50% relative humidity (RH). The instrument was equipped with a Berkovich-type diamond indenter, characterized by a three-sided pyramidal geometry, enabling local mechanical characterization of fibre cell walls.

For all samples, a maximum indentation depth of 120 nm was applied. The experimental protocol included a loading phase at a strain rate of 0.05 s^{-1}, followed by a 20-second hold at maximum load. Unloading was then performed at a constant rate of 10 μN/s.

The load-displacement curves were analysed using the method proposed by Oliver and Pharr (1992), which determines the indentation modulus from the slope of the unloading curve. This methodology, widely used for the characterization of biological materials and polymers, provides a reliable estimate of the mechanical properties of hemp fibres.

In this study, indentation modulus and hardness were calculated during the unloading stage, to avoid the influence of possible structural changes occurring during the loading phase.

For each stage of development, nanoindentation experiments were conducted on three independent stems to assess inter-stem variability. For each stem, 20 indentations were performed per fibre, and four fibres were analysed per stem, resulting in a total of 80 indentations per stem.

The indentation values were first averaged at the fibre level prior to statistical analysis to evaluate the local mechanical properties of the cell wall.

The results showed high consistency among the stems. For clarity, the data presented in this study correspond to a single representative stem, selected based on the consistency observed among the three stems. The reported indentation modulus values were obtained by averaging the measurements across the four fibres of this stem.

For the multiscale correlative analysis, the same representative stem was used for all subsequent characterizations (AFM, Raman microspectroscopy, and X-ray microtomography), thereby ensuring a consistent multiscale description of fiber structure and mechanical properties.

2.5. AFM peak force QNM measurements

Analyses were performed using a multimode atomic force microscope (AFM) (Bruker Corporation, USA) operating in Peak Force Quantitative Nanomechanical Mapping (PF-QNM) mode. A RTESPA−525 probe (Bruker), with a spring constant of 200 N/m and a tip radius of 43 nm, was used.

The probe was calibrated using the Sader method (https://sader-method.org/), resulting in optimum measurement accuracy. The tip radius, initially estimated at 43 nm, was refined during measurements using a Kevlar sample, which served as a reference material with an indentation modulus of between 18 and 20 GPa. All measurements were carried out with a scan speed of 5 μm/s and a maximum applied force of 200 nN.

For each developmental stage, AFM measurements were performed on two independent stems that had previously been used for nanoindentation to assess reproducibility. Two images were acquired per stem. Indentation modulus maps were analysed to extract local values, and both the mean and distribution of values were reported for each stage. The results showed high consistency between the stems. To ensure

consistency within the correlative multiscale framework, the AFM results presented correspond to the same representative stem selected for the nanoindentation analysis.

2.6. Raman micro-spectroscopy

Raman spectra were recorded using an InVia confocal Raman microspectrometer (Renishaw, Wotton-under-Edge, England). Confocal Raman microscopy is a sensitive surface technique with a spatial resolution up to 250–500 nm. A 785 nm laser with a power of 100 mW was used with a grating of 1200 grooves/mm. The spectra were collected between 300 and 3200 cm^{-1} at a 1 cm^{-1} resolution using an X100 objective and a slit opening of 65 µm. We collected 10 points for each stage of development. Wire 5.4 software was used to acquire and process the recorded data, in order to remove spikes and perform baseline correction. Data smoothing, vectorial normalization, and spectral averaging were performed with the Unscrambler 10.1 software (CAMO, Oslo, Norway).

Characteristic Raman bands were identified for the main fibre components, in agreement with the literature (Wiley and Atalla, 1987): cellulose and hemicellulose (400–530, 1095, 1120, 1335, 1375 cm^{-1}), crystalline cellulose (380 cm^{-1}), and lignin (1600–1630 cm^{-1}).

2.7. Statistical analysis and data treatment

To determine whether the differences observed between the groups were statistically significant, a one-way ANOVA was performed when comparing more than two developmental stages. For pairwise comparisons, a Student's *t*-test was used. When ANOVA revealed significant differences, post-hoc pairwise comparisons between stages were carried out using Tukey's HSD test. A p-value < 0.05 indicates a statistically significant difference. The results from nanoindentation and AFM were represented using box plots, following the standard representation of box plots in Excel (e.g., as described by Excelguru.com). This format displays, the interquartile range (IQR) the median and potential outliers, allowing for robust visualization of the distribution of data between different samples or stages of development.

3. Results and discussion

3.1. Evolution of stem architecture and fibre morphology along plant development

Fig. 3 illustrates the morphological evolution of hemp fibres at the three maturity stages studied (50, 80, and 122 days after sowing). There is a progressive change in fibre structure, characterized by an increase in cell wall thickness. At 122 days, the primary fibres are more developed, with a thicker secondary cell wall and a smaller lumen compared to those at 50 and 80 days, reflecting an ongoing maturation process.

This trend is quantitatively supported by Table 1 and Fig. 4(a–c), which show a consistent reduction in lumen size with increasing fibre maturity. The maximum Feret diameter of the lumen decreases from 17.2 µm at 50 days to 16.3 µm at 80 days, and reaches 10.3 µm at 122 days. A similar evolution is observed when considering the lumen area, which declines from 163 $µm^2$ at 50 days to 148 $µm^2$ at 80 days, and drops further to 57 $µm^2$ at 122 days. Despite the relatively large standard deviations, these changes are not simply the result of natural variability. The entire distributions of both lumen diameter and lumen area shift toward smaller values, demonstrating a coordinated and progressive reduction in lumen cross-section throughout development.

Importantly, this reduction does not reflect a collapse of the lumen but rather the progressive thickening of the fibre walls associated with secondary wall deposition. As the wall layers accumulate, the internal cavity is gradually constricted, leading to smaller lumen diameters and areas. The combined analysis of these two metrics therefore provides a coherent and robust anatomical signature of fibre maturation, directly linked to the dynamics of wall thickening.

Simultaneously, as shown in Fig. 4(c), the cell wall thickness increases with maturity, suggesting that the fibres progressively fill inward with wall material mainly cellulose and non-cellulosic polymers

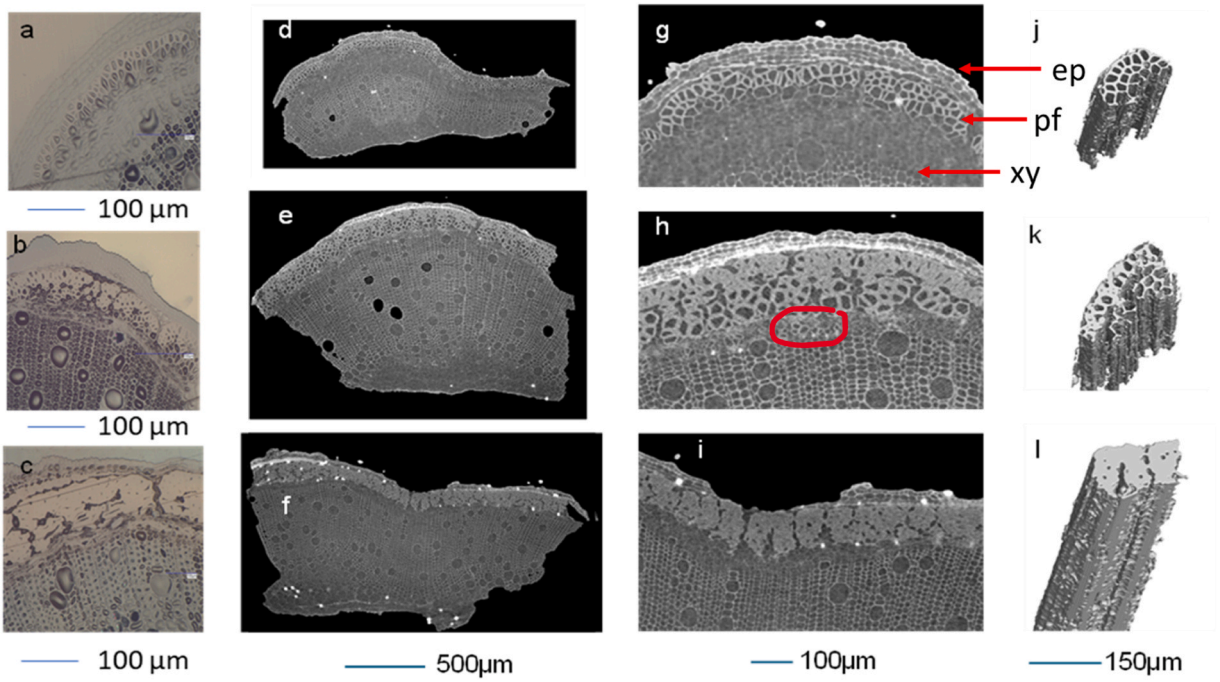

Fig. 3. Optical microscopy and X-ray tomography of hemp stems at three developmental stages (50,80, and 122 days). Observations were performed on one stem per stage, sampled at the middle region of the stem. a, b, c: Optical microscopy images. d, e, f: Transverse cross-sections obtained by X-ray tomography. g, h, i: Zoomed views of the transverse tomography sections; in h, areas circled in red may correspond to possible secondary fibres. j, k, l: 3D representations of fibres virtually extracted from the stem. Developmental stages: a, d, g, j: Primary fibres at 50 days; poorly developed, thin walls, large lumen. b, e, h, k: Fibres at 80 days; intermediate development. c, f, i, l: Fibres at 122 days; fully mature with thickened cell walls. Abbreviations: Ep: epidermis; pf: primary fibre; xy: xylem.

Table 1
Mean values and standard deviations of morphological parameters (lumen area, maximum Feret diameter, minimum Feret diameter, and fibre wall thickness) measured at threedevelopmental stages (50, 80, and 122 days). For each stage, one stem was analysed. Values shown represent the mean per stem.

Maturity	stem analysed	Number of analysed fibres	Lumen area (μm^2)	Lumen max diameter (μm)	Lumen min diameter (μm)	Fibre wall thickness (μm)
50 days	1	102	163 ± 95	17.2 ± 6.5	10.4 ± 4.3	4.8 ± 0.8
80 days	1	105	148 ± 110	16.3 ± 8.9	9.8 ± 5.7	6.7 ± 1.7
122 days	1	62	57 ± 50	10.3 ± 5	6.4 ± 2.5	8.6 ± 2.5

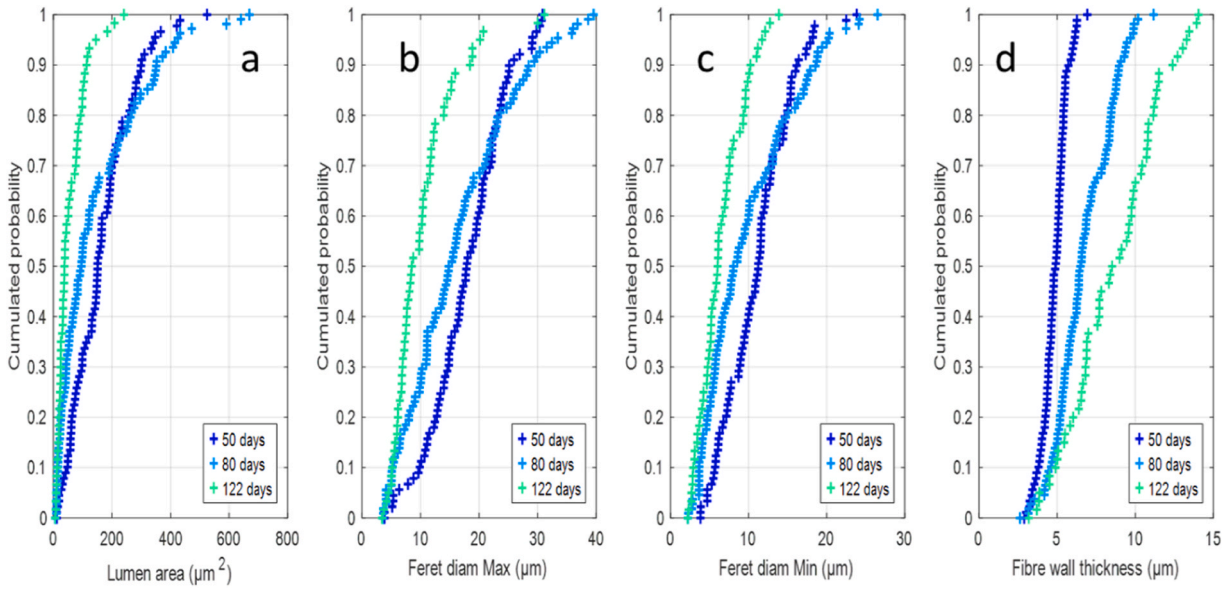

Fig. 4. Cumulative probabilities of the morphological detection from tomographic images for 4 parameters. (a) for the lumen area in μm^2, (b) for the Feret maximum lumen diameter, (c) for the Feret minimum lumen diameter and (d) for the fibre wall thickness. For each stage, one stem was analysed.

while the outer fibre diameter remains relatively constant. This observation reinforces the idea of a maturation-driven reinforcement process, where fibres do not expand externally but densify internally.

Further insights are provided by Fig. 5, which plots the wall thickness of fibres as a function of their radial position in the stem. At 50 and 80 days of maturity, fibres closer to the stem periphery exhibit noticeably thicker walls than those nearer the center. This spatial variation may reflect a radial gradient of fibre maturation, with peripheral fibres initiating the thickening phase earlier than those closer to the core. This pattern supports the hypothesis of centripetal maturation of hemp fibres, meaning that fibres located at the periphery of the stem begin thickening earlier than those closer to the center. This outward to inward progression is accompanied by a progressive deposition of the secondary cell wall, similar to the dynamics observed in flax (Gorshkova et al., 2003). These observations are also consistent with Kim et al. (2021), who reported a progressive increase in secondary wall thickness in hemp fibres during their maturation.

Very few secondary fibres were observed in the analysed samples. However, some structures are briefly visible at 80 days (Fig. 3h, circled in red), suggesting the presence of a small proprotion of secondary fibres. Quantification of their surface area, compared with that of primary fibres, shows that secondary fibres represent only 6% of the total fibre fraction, which is low compared with previously published studies (Snegireva et al., 2015). Their limited presence can be explained by the fact that the sections studied here were taken from the middle part of the stem, whereas secondary fibres, which provide additional mechanical support during plant growth, are generally more abundant in the lower part of the stem (Snegireva et al., 2015).

3.2. Development of cell wall mechanical during hemp stem development

The mechanical properties of hemp fibre cell walls were analysed using nanoindentation, allowing the measurement of indentation modulus and hardness. Analysis of fibres at the three developmental stages revealed a progressive increase in both indentation modulus and hardness during maturation (Fig. 6).At 50 days, the indentation modulus of fibres was 16.7 ± 1.9 GPa, increasing to 18.0 ± 1.6 GPa at 80 days and 21.5 ± 2.1 GPa at 122 days (Fig. 6a). One-way ANOVA revealed a significant effect of developmental stage ($p < 0.05$), and Tukey's HSD test indicated significant differences between all stages.

Regarding hardness (Fig. 6b), the mean value was 342 ± 57 MPa at 50 days, followed by a slight increase to 350 ± 33 MPa at 80 days, with no statistically significant difference between these stages (one-way ANOVA, $p > 0.05$). In contrast, a significant increase was observed at 122 days, with a hardness of 429 ± 57 MPa ($p < 0.05$, Tukey's HSD test). These results indicate that the cell walls become progressively stiffer and harder as the fibres mature. The indentation modulus and hardness are indicative of the behaviour of cellulose microfibrils and non-cellulosic polymers, respectively (Eder et al., 2013). Hardness is particularly influenced by non-cellulosic polymers (such as pectins and hemicelluloses in the case of hemp fibres). The gradual increase in hardness during development suggests a structural reinforcement of the cell walls, likely linked to the accumulation of polysaccharides. As observed in the indentation analysis, these non-cellulosic components are expected to contribute to fibre stiffening and enhance their mechanical strength.

These observations are consistent with those reported in flax by (Goudenhooft et al., 2018), who showed that the transition to mature fibres is accompanied by changes in cell wall composition, with a gradual shift from a galactan-enriched Gn layer to a more homogeneous and compact G layer that is less rich in galactans, thereby contributing to increased fibre stiffening during maturation.

Similarly, (Gorshkova and Morvan, 2006) highlighted the crucial role of galactans in the early stages of fibre development, with their

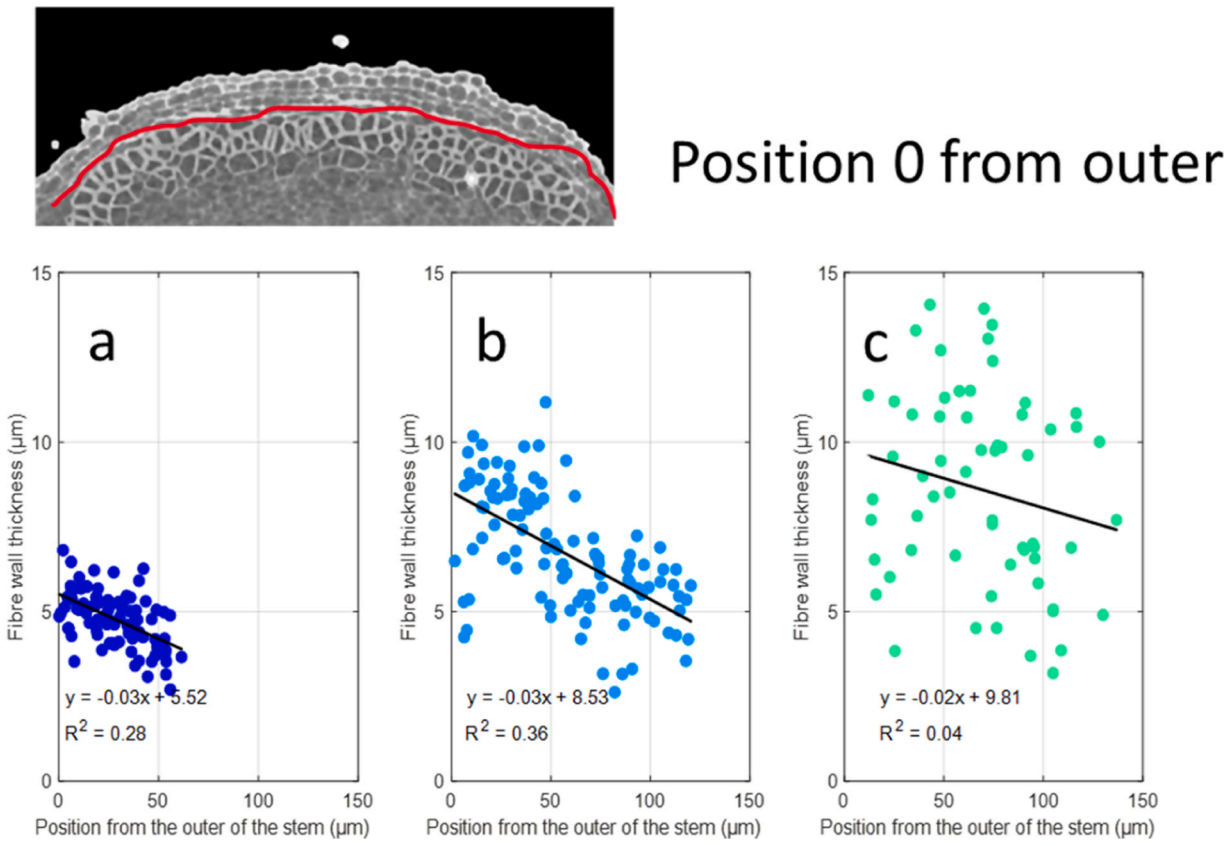

Fig. 5. Values of the fibre wall thickness as a function of the position from the stem periphery. a for 50 days stem, b for 80 days stem and c for 122 days stem. For each stage, one stem was analysed.

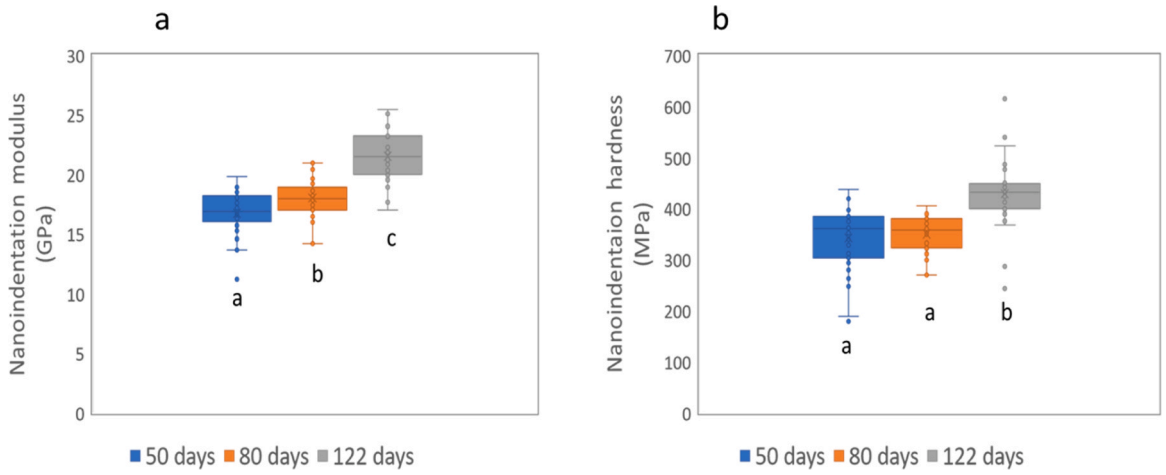

Fig. 6. Nanomechanical properties of hemp cell walls at three developmental stages (50, 80, and 122 days) obtained by nanoindentation: (a): Nanoindentation modulus (NI). (b): Nanoindentation hardness. The box plots represent the distribution of values obtained from 20 indentations per fibre, performed on 4 individual fibres. Boxes with different superscript letters (a, b, c) indicate statistically significant differences between groups ($p < 0.05$, one-way ANOVA followed by Tukey's post-hoc test). All assays were performed on one stem per developmental stage.

progressive reduction being associated with the formation of the gelatinous layer (G-layer) and fibre stiffening.

These results emphasize the key role of non-cellulosic polymers in the mechanical resistance of plant cell walls and confirm that their evolution directly influences fibre properties.

The mechanical properties of hemp fibres were also characterized by AFM-PF-QNM to complement the nanoindentation analysis (Fig. 6), offering a comparable measurement mode with higher spatial resolution. Measurements were performed on the same fibres, enabling direct comparison between the two techniques.

The modulus obtained by AFM PF-QNM follows a similar trend to that measured by nanoindentation, confirming a progressive increase in mechanical properties during fibre development. Using nanoindentation, indentation moduli were found to be 16.7 ± 1.9 GPa at 50 days, 18.0 ± 1.6 GPa at 80 days, and 21.5 ± 2.1 GPa at 122 days (Fig. 6).

AFM PF-QNM measurements revealed comparable values, with an indentation modulus of 15.7 ± 1.5 GPa at 50 days. One-way ANOVA

indicated a significant effect of developmental stage ($p < 0.05$), with a marked increase to 19.6 ± 1.6 GPa at 80 days and a further rise to 20.6 ± 1.9 GPa at 122 days (Fig. 7). Tukey's HSD test confirmed that the differences between all stages were statistically significant ($p < 0.05$).

These results highlight the progressive stiffening of cell walls associated with fibre maturation and demonstrate a similar increase in modulus measured by both AFM and nanoindentation, confirming the complementarity of the two techniques. However, these methods differ in terms of spatial resolution and indentation depth. Nanoindentation exhibits a greater indentation depth (approximately 120 nm), allowing a larger interaction volume to be probed and providing an averaged mechanical response over a deeper region of the cell wall. In contrast, AFM offers higher spatial resolution and a much smaller indentation depth (approximately 2–3 nm), enabling the measurement of mechanical properties at the nanoscale and the detection of local heterogeneities within the cell wall. Thus, AFM allows fine mapping of mechanical properties, whereas nanoindentation provides local mechanical characterization at a slightly larger scale.It is important to note that both techniques rely on model assumptions that can influence the measured modulus. AFM-PF-QNM measurements depend on the chosen contact model; in this study, the DMT model was used to estimate the contact modulus, assuming a linearly elastic and isotropic material. The reported values therefore correspond to the contact modulus under these assumptions. Calibration of the AFM tip (tip radius, cantilever sensitivity, spring constant) was performed prior to each measurement series to minimize systematic errors.For nanoindentation, the modulus is calculated according to the Oliver-Pharr model, which assumes a homogeneous and isotropic material at the scale of the indentation. This assumption may introduce biases when measuring heterogeneous cell walls, particularly at early stages of fibre maturation. Additionally, indentation depth was chosen to remain below 10–20% of the cell wall thickness to limit the influence of the lumen or substrate. Nevertheless, at early stages, when the walls are very thin, proximity effects of the lumen or resin infiltration can influence the measured values, representing a limitation to be considered when interpreting the data.

Boxes with different superscript letters (a, b, c) indicate statistically significant differences between groups ($p < 0.05$, one-way ANOVA followed by Tukey's post-hoc test)

AFM PF-QNM images (Fig. 8) also enable the analysis of morphological variations in fibres as a function of their developmental stage. Progressive thickening of the cell wall is clearly observed, accompanied by a corresponding reduction in lumen size, which becomes very small after 122 days, consistent with enhanced mechanical performance.

3.3. Progressive evolution of the compound middle lamellae

The compound middle lamella (CML) is an intercellular structure that ensures the cohesion of adjacent plant cells. It is located between the primary walls and plays a key role in cell adhesion (Zamil and Geitmann., 2017).

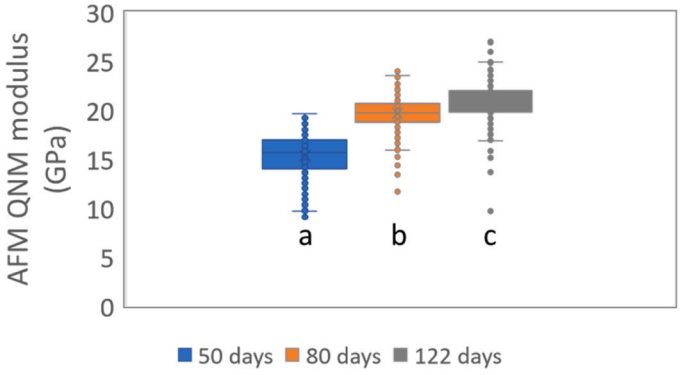

Fig. 7. AFM QNM modulus of hemp fibres at three developmental stages (50, 80, 122 days). Boxplots represent the distribution of modulus values measured point by point within a single fibre per developmental stage, illustrating local variability along the cell wall.

In the present study, its mechanical evolution was monitored during hemp fibre maturation using AFM PF-QNM. Fig. 9 shows the AFM QNM modulus maps obtained for samples at 50, 80, and 122 days of development, along with the corresponding AFM QNM modulus distributions for the central lamella region. These results reveal a progressive increase in CML stiffness during development.

At 50 days after sowing, the CML exhibits a relatively homogeneous structure and low stiffness, with an average indentation modulus of 7.1 ± 0.7 GPa. The distribution of values is narrow and centered around 7 GPa. At 80 days, a significant increase in modulus is observed ($p < 0.05$), reaching an average of 10.8 ± 0.8 GPa. This increase is accompanied by a moderate broadening of the distribution, suggesting growing heterogeneity in mechanical properties.

At 122 days, ML stiffness increases even more markedly, with a mean modulus of 13.6 ± 2.2 GPa, significantly higher than that measured at 80 days ($p < 0.05$). The wider distribution at this stage reflects increased structural variability, likely linked to cell wall maturation and reorganisation processes. The values are comparable to those reported by (Melelli et al., 2020) for the middle lamellae of hemp. Our results show a correlation between fibre development and ML strengthening, probably linked to progressive densification of the extracellular matrix, associated with lignification of cell wall. Understanding the progressive stiffening of this zone is essential. (Fuentes et al., 2017) showed that technical fibres with strong cohesion, richer in substituted pectins, exhibit better mechanical performance than those with weaker cohesion, thus highlighting the key role of this interfacial zone in the mechanical behaviour of fibres.

3.4. Heterogeneity of fibre maturation

Morphological heterogeneity is observed among fibres at different developmental stages. At 50 days, most fibres exhibit thin cell walls associated with large lumens, as illustrated by the lumen area distribution (Fig. 10). However, some fibres display a markedly reduced lumen, indicating early thickening of the secondary cell wall. This pattern highlights an asynchronous maturation process, in which some fibres rapidly progress toward a mature state while others remain at an earlier stage of development.

To clarify this distinction, these early-maturing fibres are referred to here as "filled fibres", characterized by a strongly reduced lumen due to pronounced secondary wall thickening. A fibre is considered filled when its lumen represents 9–16% (or less) of the total cross-sectional area, a threshold consistent with values reported in the literature for mature hemp fibres (Schäfer and Honermeier, 2006).

Based on this criterion, a threshold value of 15% for lumen area was defined, and the proportion of filled fibres (i.e., fibres with a lumen area below 15% of the total fibre area) was estimated at approximately **3.9%** (Table 2) at 50 days, indicating the early presence of a fraction of fibres already advanced in maturation. This proportion increases to **32.3%** (Table 2) at 80 days, reflecting the progressive thickening of the cell wall during development. At 122 days, corresponding to a stage close to seed maturity, the majority of fibres (**80.7%**; Table 2) exhibit a strongly reduced lumen, characteristic of a fully mature state.

Mechanical analysis of these filled fibres at 50 days reveals distinct properties: their indentation modulus reaches 19.7 ± 0.5 GPa in nanoindentation, with a hardness of 369 ± 12 MPa, while AFM-PF-QNM measurements give a modulus of 19.5 ± 2.5 GPa.

Compared with unfilled fibres at the same developmental stage (50 days) (Fig. 11), filled fibres show a significantly higher indentation modulus (nanoindentation, data not shown) and a higher modulus measured by AFM PF-QNM ($p < 0.05$) (Fig. 11c). These values, close to those of fibres sampled at 80 and 122 days, suggest that some fibres at 50 days reach advanced mechanical properties at an early stage, in contrast

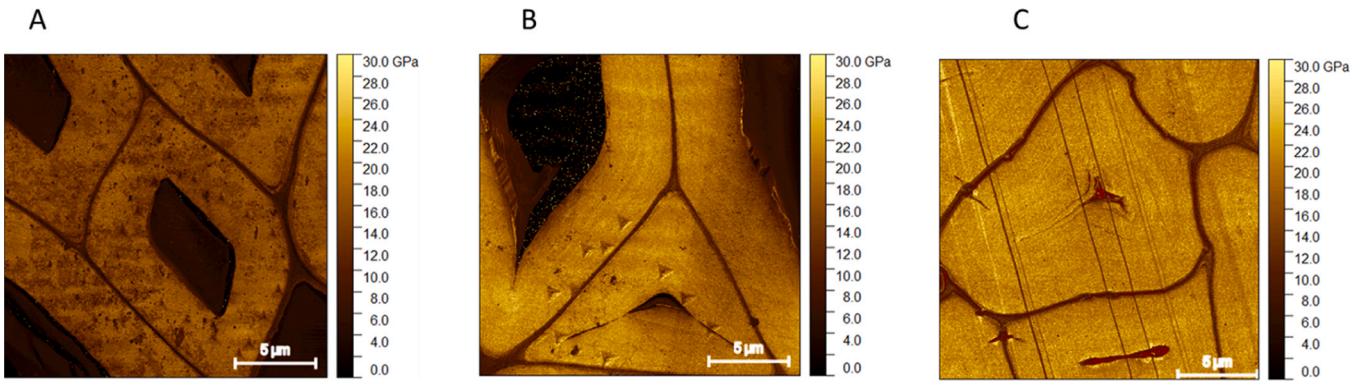

Fig. 8. AFM-PF-QNM modulus mapping of the hemp fibre walls at different stages of development. (A) 50 days, (B) 80 days, and (C) 122 days. Each image corresponds to a 384 × 384 pixel map, where each pixel represents a local modulus measurement obtained from force-distance curves.

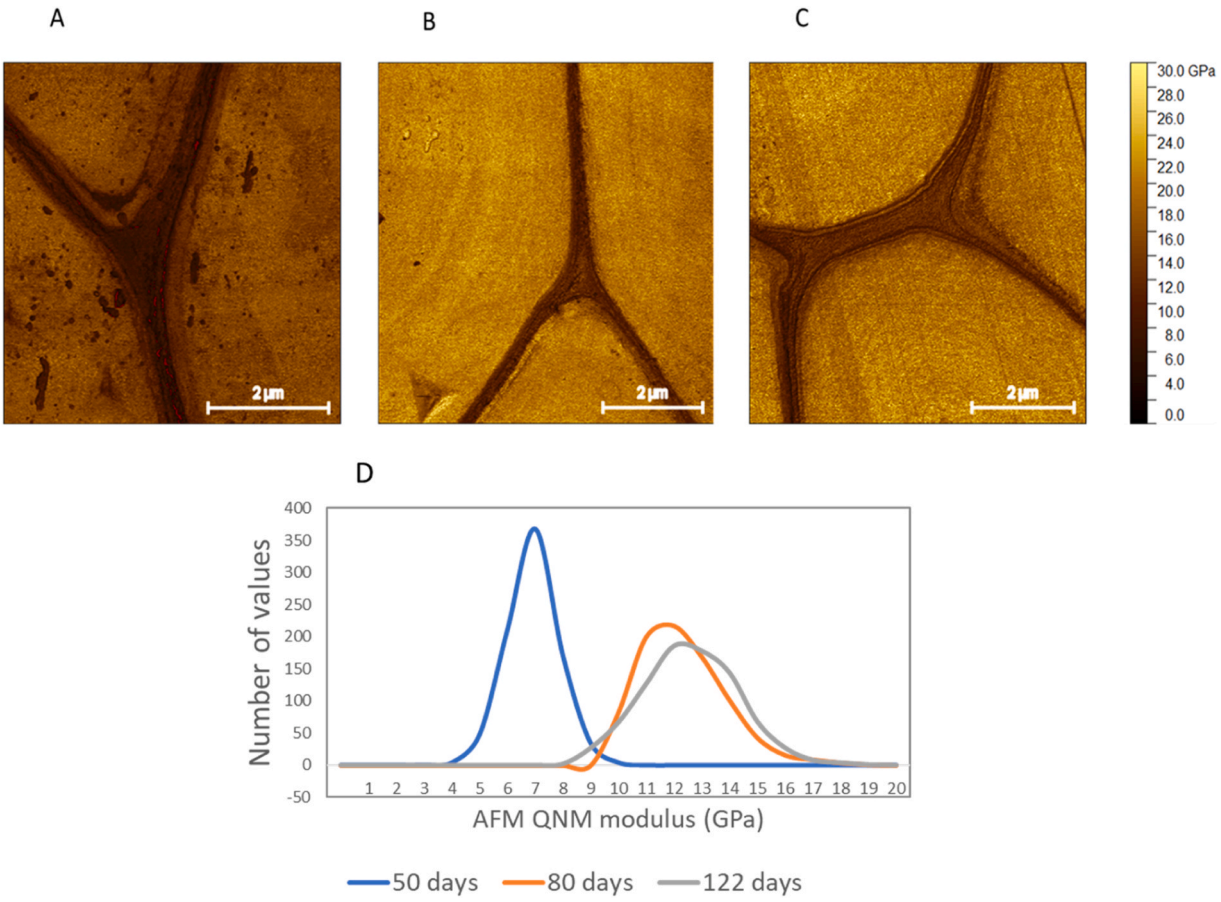

Fig. 9. Evolution of the AFM QNM modulus of ML during hemp fibre maturation. (A-C): AFM QNM modulus mappings of ML at the three developmental stages.: (A) 50 days, (B) 80 days, and (C) 122 days. (D): Corresponding distributions of AFM QNM modules extracted specifically from areas of the middle lamella for each stage. (A) 50 days, (B) 80 days, and (C) 122 days. Images are 384 × 384 pixels.

to fibres that are still developing at the same stage.

The coexistence, within a single bundle, of mechanically mature and immature fibres may have mechanical implications and could influence the overall mechanical behaviour of the stem, particularly during the early stages of development. More generally, this asynchronous maturation highlights the importance of taking into account the distribution of fibre maturity stages within the stem.

From an application perspective, these results demonstrate that fibre maturation is a key determinant of mechanical performance. Consequently, for applications requiring high mechanical properties, harvesting at a late developmental stage, close to seed maturity, appears to be the most suitable strategy, as it maximizes the proportion of mechanically mature fibres.

AFM PF-QNM can reveal gradients in mechanical properties and areas of heterogeneity within the fibre cell wall. This heterogeneity is particularly visible on the AFM QNM modulus mapping (Fig. 12), where it manifests as low modulus regions, which appear as slightly darker or lower-contrast areas. These variations in contrast reflect local differences in stiffness.

The distribution of AFM QNM modulus for filled fibre at 50 days (orange curve Fig. 12) shows marked variability, with values ranging from 10 GPa to over 24 GPa. Notably, some regions of the cell wall reach

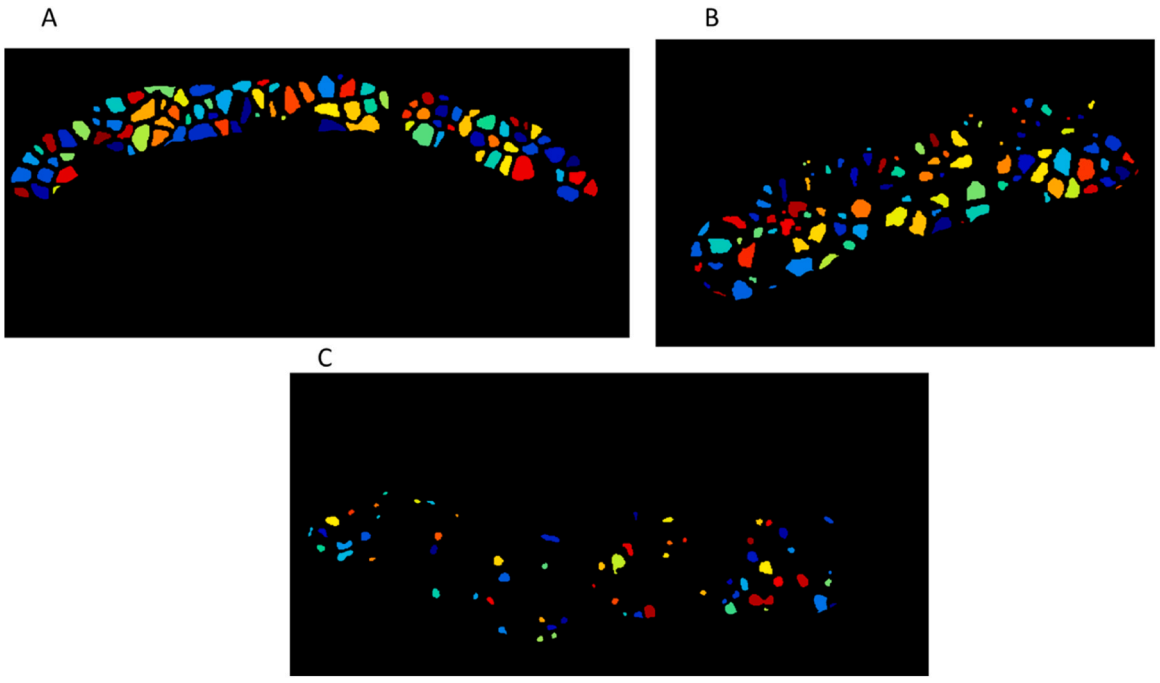

Fig. 10. Illustration of the segmentation of fibre lumens in cross-sections at the three developmental stages studied: (A): 50 days. (B): 80 days. (C): 122 days. Observations were performed on one stem per stage.

Table 2
Evolution of filled fibres and lumen proportion during fibre maturation. For each stage, one stem was analysed.

Maturity	Stem analysed	Number of analysed fibres	Number of filled fibres	Percentage of filled fibres	Average lumen Size (%)
50 days	1	102	4	3.9 %	35.9 %
80 days	1	105	34	32.4 %	24.3 %
122 days	1	62	50	80.7 %	10.67 %

high values, sometimes comparable to those observed in more mature fibres sampled at 80 and 122 days. The modulus distribution for filled fibres at 50 days exhibits two distinct maxima, indicating the presence of two populations within the fibre. This bimodality may reflect non-homogeneous maturation, with certain regions already exhibiting higher moduli characteristic of a more advanced developmental stage. It may also result from an uneven distribution of cell wall components, suggesting that the maturation process is still ongoing.

These results suggest that, although at an earlier stage of development overall, some fibres at 50 days already exhibit locally very stiff regions, indicative of advanced mechanical maturation. This partial maturity contrasts with the relative homogeneity observed in unfilled fibres at the same age, whose modulus remains generally lower and more uniform.

This heterogeneity may reflect non-uniform cell wall maturation within a single fibre cross-section. It can be explained by the progressive action of galactosidase enzymes, which are responsible for the breakdown of galactan chains and, consequently, for the gradual stiffening of the cell wall, given the key role of these polymers in cell wall cohesion and structure (Goudenhooft et al., 2018; Gorshkova Morvan, 2006).

Compared with previous studies, notably in hemp (Kim et al., 2021)

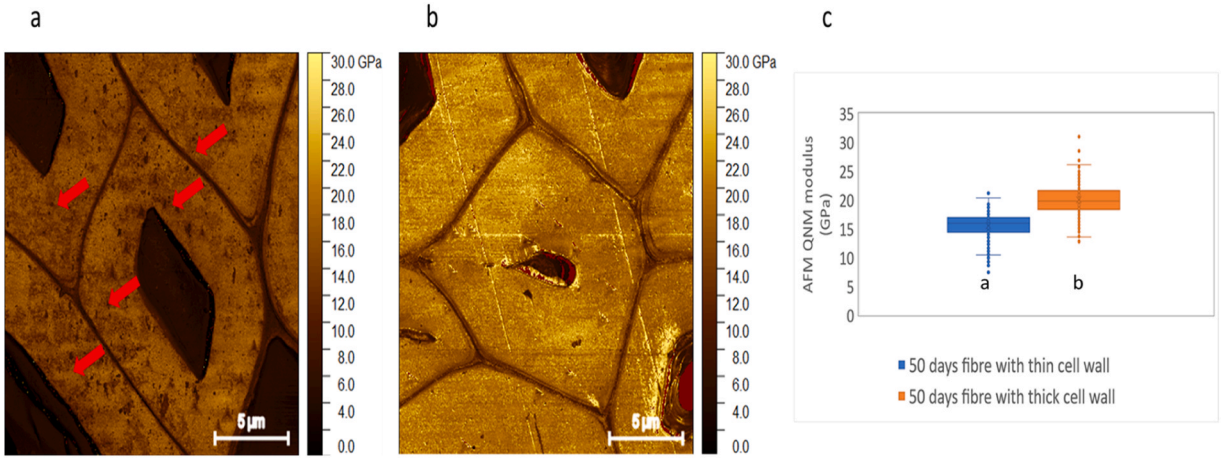

Fig. 11. Comparison of unfilled and filled fibres at 50 days. (a): AFM QNM modulus mapping of a 50-day unfilled fibre. Red arrows indicate these low-modulus regions. (b): AFM QNM modulus mapping of a 50-day filled fibre with a smaller lumen. (c): Comparison of AFM QNM modulus for the unfilled 50-day fibre and the filled 50-day fibre. Boxes with different superscript letters (a, b) indicate statistically significant differences ($P < 0.05$). Images are 384 × 384 pixels.

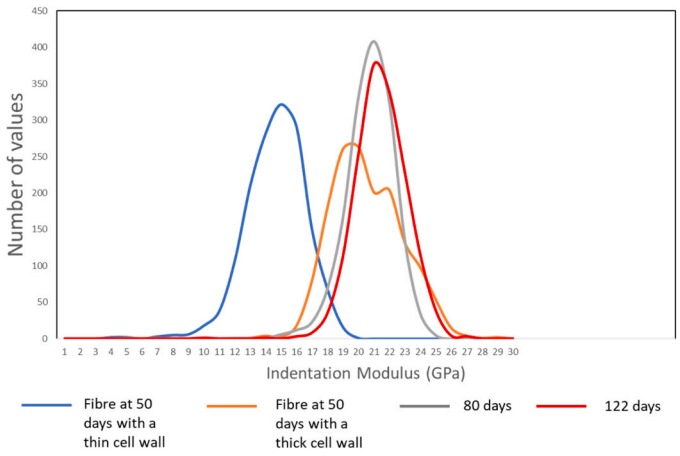

Fig. 12. AFM-PF-QNM modulus distribution of hemp fibres at three developmental stages.

and flax (Goudenhooft et al., 2018), we were unable to definitively identify the presence of Gn layers during fibre maturation. Analyses performed on fibres from the middle part of the stem at 50 and 80 days did not reveal structures exhibiting the typical characteristics of Gn layers. However, certain mechanically heterogeneous zones observed in fibres at 50 days display features that could suggest the presence of such structures, although it is not possible to draw a definitive conclusion regarding their presence at this stage.

3.5. Raman spectroscopy investigations

Mean Raman spectra are shown in Fig. 13. These spectra reveal bands attributed to the three main fibre components: cellulose and hemicelluloses at 400–530, 1095, 1120, 1335, and 1375 cm^{-1} ; crystalline cellulose at 380 cm^{-1} ; and lignin at 1600–1630 cm^{-1} , as previously reported in the literature (Wiley and Atalla; 1987). Interestingly, we observe an increase in the more specific cellulose peak intensities (380 and 1375 cm^{-1}) as a function of the maturation stage, consistent with higher cellulose content at the mature stage. The increase in peaks from 440 to 530 cm^{-1} , 1095 cm^{-1} , and 1120 cm^{-1} , all assigned to both cellulose and hemicellulose, clearly correlates with and supports the increase in nanoindentation modulus and hardness highlighted in the previous sections. The mechanical and tensile properties of many bio-based composites are known to be highly sensitive to cellulose content (Mathel et al., 2025; Nuez et al., 2020), as well as at the cell wall scale (Del Masto et al., 2019). Regarding the hemicellulose component, we note a higher intensity of the band at 570 cm^{-1} . As we calculate a decrease in the I_{494}/I_{570} ratio, an indicator of increased substitution of

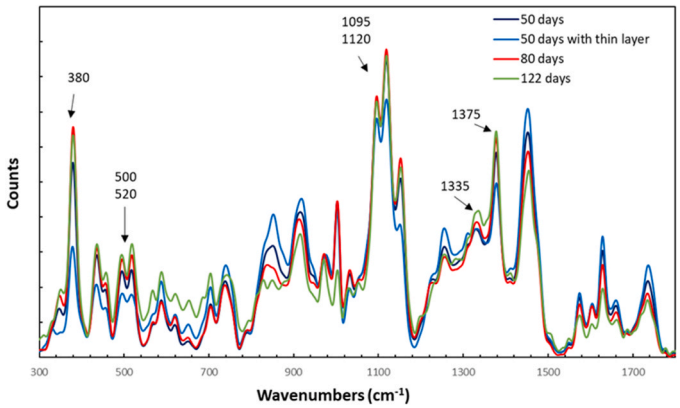

Fig. 13. Mean Raman spectra of hemp fibres at three developmental stages.

xylan by arabinose residues, we can expect a higher degree of substitution of the xylan backbone by arabinose side groups. It has been proved, in literature (Mathel et al., 2025), that the arabinoxylan polymer stiffness increases with their substitution degree, mainly due to the higher glass transition. Furthermore, this substitution induces increased branching and the removal of hydrophilic groups, resulting in fewer hydrogen bonds between water (Ying et al., 2011) and the arabinoxylan chains, as well as a less mobile backbone, thereby promoting stiffening. Literature report that xylan more branched by arabinose side groups have brittle behavior when manufactured for film packaging (Ying et al., 2015). In the cell wall, a remodeling of the arabinoxylan toward more branched polymers would certainly favor less water molecules interactions and concomitantly higher stiffness of the polymer network.

These observations are confirmed by the principal component analysis (Fig. 14). PC1 explains 56% of the total variance in the dataset and discriminates samples according to their developmental stage. The corresponding loading plot, which allows the identification of relevant wavenumbers, assigns positive values to the main compositional features of the 80- and 122-day samples. It highlights compositional changes related to cellulose and hemicellulose contents, which are higher in the older samples. This analysis reveals an increase in crystalline cellulose from 50 to 80 days, which then stabilizes at the mature stage.Raman measurements were used to estimate the cellulose crystallinity index, following the adapted method of (Agarwal et al., 2010). Fibres at 50 days showed relatively low crystallinity (41%), whereas fibres collected at 80 and 122 days reached high values (87–88%), corresponding to an advanced stage of maturation.

As mentioned above, at 50 days, fibres exhibited heterogeneity. Both thin-walled fibres with large lumens and thick-walled fibres, referred to as “filled fibres” with strongly reduced lumens, were observed. These filled fibres showed higher crystallinity (75 %) and a significantly higher indentation modulus compared to thin-walled fibres at the same stage. This confirms that some fibres reach near-mature mechanical and biochemical properties at an early developmental stage.

However, this difference remains relative: the crystallinity and modulus of filled fibres at 50 days are still lower than those of fibres observed at 80 and 122 days, indicating that even early-developing fibres are not yet fully mature. This observation highlights the asynchronous and heterogeneous nature of fibre maturation within a single developmental stage.

It should be noted that all analyses were performed on fibres from the same stem, ensuring that the measured trends are comparable across techniques at the stem level. However, mechanical measurements (AFM PF-QNM and nanoindentation) were conducted on the same fibres, whereas optical microscopy, Raman spectroscopy, and tomography were performed on different fibres from the same stem. Despite this limitation, a clear positive correlation is observed between cellulose crystallinity and the indentation modulus measured by nanoindentation, as illustrated in Fig. 15.

Therefore, quantitative correlations between mechanical properties and morphological or chemical data can only be assessed at the stem or regional level, rather than on the exact same fibres. This limitation should be taken into account when interpreting the results obtained from the different techniques.

4. Conclusion

Hemp fibre maturation involves progressive and coordinated cell wall transformations at the structural, mechanical, and biochemical levels, which directly influence their properties.

In this study, we demonstrated that the evolution of cell wall composition, particularly cellulose and hemicellulose, is associated with a significant increase in the indentation modulus measured by nanoindentation and AFM-PF-QNM. At 50 days, fibres exhibit thin cell walls and low modulus, while cell wall thickening, initiated at 80 days along with lumen reduction, continues until 122 days at which point fibres

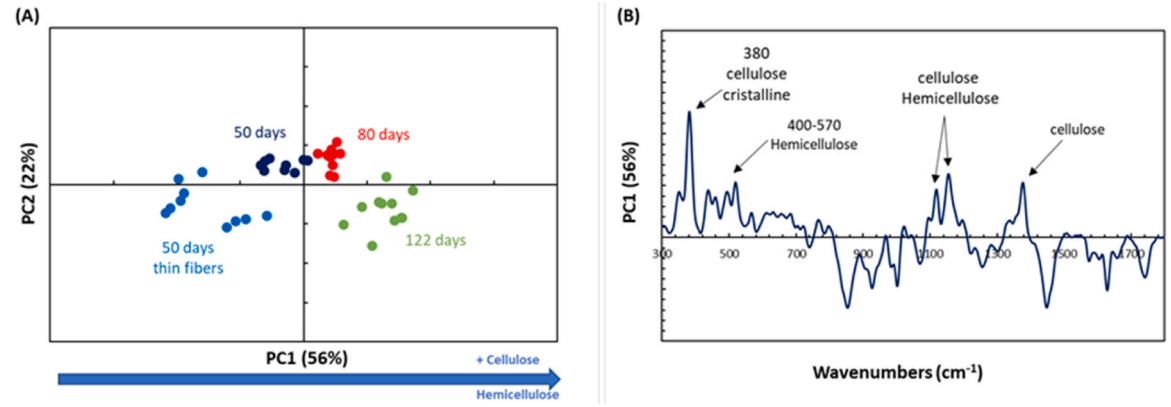

Fig. 14. Principal Component Analysis: Scores plot (A) and loadings plot for PC1 (B).

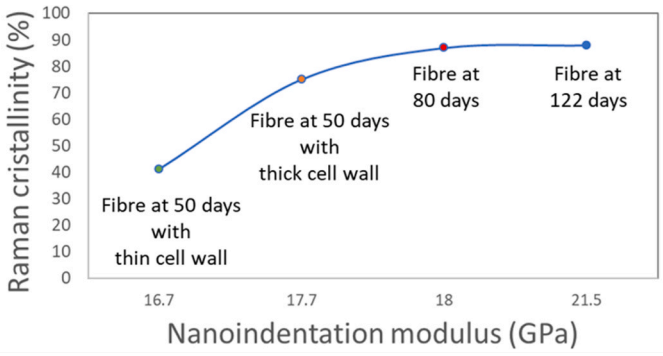

Fig. 15. Correlation between cellulose crystallinity measured by Raman spectroscopy and indentation modulus obtained by nanoindentation on the same stem.

display dense walls, reduced lumen, and enhanced mechanical properties.

The use of these techniques allowed us to demonstrate that morphological changes (wall thickening and lumen reduction) are accompanied by an increase in cell wall mechanical properties, as expected. We also observed that stem filling occurs from the outer to the inner regions, as previously reported for flax. Raman spectroscopy showed that mechanically advanced fibres have a higher degree of cellulose crystallinity and a more mature biochemical composition confirming the link between structure, mechanics, and chemistry. Notably, we observed heterogeneity in fibre maturation. At 50 days, most fibres have thin walls and large lumens, while some fibres (3,9%) exhibit thicker walls and are designated as “filled fibres”. This asynchronous maturation is particularly important to understand. The proportion of filled fibres increases from 3,9% at 50 days to 32,4% at 80 days and reaches 80,7% at 122 days, where nearly all fibres are filled with thick walls and reduced lumen.

This maturation dynamic is crucial for applications such as textile or composite preforms development requiring high mechanical performance fibres, as it provides insights into the optimal harvesting window to maximize the proportion of mature fibres. Understanding the asynchronous and heterogeneous nature of fibre maturation is therefore essential for optimizing hemp fibre properties.

Declaration of Competing Interest

The authors declare that they have no known competing financial interests or personal relationships with other people or organizations that could have appeared to influence the work reported in this paper.

Acknowledgements

The authors gratefully acknowledge the ANR (Agence Nationale de la Recherche) for funding the TAFFTA project (ANR−23-CE51–0061 – TAFFTA), as well as the EIPHI Graduate School (ANR−17-EURE−0002). The authors are grateful to Lucie Le-Bot (INRAE) for fruitful discussions. They also thank Mary Charles Bray and Rigoberto Ibarra Gomez for their careful proofreading and English editing. The authors further acknowledge the MIFHySTO technological platform (FEMTO-ST, France) for support with X-ray nanotomography characterization, and the BIBS instrumental platform (http://www.bibs.inrae.fr/bibs_eng/, UR1268 BIA, IBiSA, PROBE infrastructure, Biogenouest) for Raman measurements. Finally, the authors would like to thank the “Drôme Chanvre” association (Piegros-La-Clastre, France) for providing hemp stems (Cannabis sativa L., variety Santhica 70).

References

Agarwal, U.P., Reiner, R.S., Ralph, S.A., 2010. Cellulose I crystallinity determination using FT–Raman spectroscopy: univariate and multivariate methods. Cellulose 17, 721–733. https://doi.org/10.1007/s10570-010-9420-z.

Andersons, J., Spārniņš, E., Joffe, R., Wallström, L., 2005. Strength distribution of elementary flax fibres. Compos. Sci. Technol. JNC13-AMAC-Strasbg. 65, 693–702. https://doi.org/10.1016/j.compscitech.2004.10.001.

Arnould, O., Arinero, R., 2015. Towards a better understanding of wood cell wall characterisation with contact resonance atomic force microscopy. Compos. Part A Appl. Sci. Manuf. 74, 69–76. https://doi.org/10.1016/j.compositesa.2015.03.026.

Aziz, S.H., Ansell, M.P., 2004. The effect of alkalization and fibre alignment on the mechanical and thermal properties of kenaf and hemp bast fibre composites: Part 1 – polyester resin matrix. Compos. Sci. Technol. 64, 1219–1230. https://doi.org/10.1016/j.compscitech.2003.10.001.

Baley, C., 2002. Analysis of the flax fibres tensile behaviour and analysis of the tensile stiffness increase. Compos. Part A Appl. Sci. Manuf. 33, 939–948. https://doi.org/10.1016/S1359-835X(02)00040-4.

Beaugrand, J., Nottez, M., Konnerth, J., Bourmaud, A., 2014. Multi-scale analysis of the structure and mechanical performance of woody hemp core and the dependence on the sampling location. Ind. Crops Prod. 60, 193–204. https://doi.org/10.1016/j.indcrop.2014.06.019.

Bos, H.L., Donald, A.M., 1999. situ ESEM study of the deformation of elementary flax fibres. J. Mater. Sci. 34, 3029–3034. https://doi.org/10.1023/A:1004650126890.

Bourmaud, A., Beaugrand, J., Shah, D.U., Placet, V., Baley, C., 2018. Towards the design of high-performance plant fibre composites. Progress. Mater. Sci. 97, 347–408. https://doi.org/10.1016/j.pmatsci.2018.05.005.

Bourmaud, A., Malvestio, J., Lenoir, N., Siniscalco, D., Habrant, A., King, A., Legland, D., Baley, C., Beaugrand, J., 2017. Exploring the mechanical performance and in-planta architecture of secondary hemp fibres. Ind. Crops Prod. 108, 1–5. https://doi.org/10.1016/j.indcrop.2017.06.010.

Chernova, T.E., Mikshina, P.V., Salnikov, V.V., Ibragimova, N.N., Sautkina, O.V., Gorshkova, T.A., 2018. Development of distinct cell wall layers both in primary and secondary phloem fibers of hemp (Cannabis sativa L.). Ind. Crops Prod. 117, 97–109. https://doi.org/10.1016/j.indcrop.2018.02.082.

Clair, B., Gril, J., Baba, K., Thibaut, B., Sugiyama, J., 2005. Precautions for the structural analysis of the gelatinous layer in tension wood. IAWA J. 26, 189–195. https://doi.org/10.1163/22941932-90000110.

Crônier, D., Monties, B., Chabbert, B., 2005. Structure and chemical composition of bast fibers isolated from developing hemp stem. J. Agric. Food Chem. 53, 8279–8289. https://doi.org/10.1021/jf051253k.

Del Masto, A., Trivaudey, F., Guicheret-Retel, V., Placet, V., Boubakar, L., 2019. Investigation of the possible origins of the differences in mechanical properties of hemp and flax fibres: a numerical study based on sensitivity analysis. Compos. Part A Appl. Sci. Manuf. 124, 105488. https://doi.org/10.1016/j.compositesa.2019.105488.

van der Werf, H.M.G., Wijlhuizen, M., de Schutter, J.A.A., 1995. Plant density and self-thinning affect yield and quality of fibre hemp (Cannabis sativa L.). Field Crops Res. 40, 153–164. https://doi.org/10.1016/0378-4290(94)00103-J.

Duval, A., Bourmaud, A., Augier, L., Baley, C., 2011. Influence of the sampling area of the stem on the mechanical properties of hemp fibers. Mater. Lett. 65, 797–800. https://doi.org/10.1016/j.matlet.2010.11.053.

Eder, M., Arnould, O., Dunlop, J.W.C., Hornatowska, J., Salmén, L., 2013. Experimental micromechanical characterisation of wood cell walls. Wood Sci. Technol. 47, 163–182. https://doi.org/10.1007/s00226-012-0515-6.

Fuentes, C.A., Willekens, P., Petit, J., Thouminot, C., Müssig, J., Trindade, L.M., Van Vuure, A.W., 2017. Effect of the middle lamella biochemical composition on the non-linear behaviour of technical fibres of hemp under tensile loading using strain mapping. Composites Part A: Applied Science and Manufacturing 101, 529–542. https://doi.org/10.1016/j.compositesa.2017.07.017.

Gorshkova, T., Brutch, N., Chabbert, B., Deyholos, M., Hayashi, T., Lev-Yadun, S., Mellerowicz, E.J., Morvan, C., Neutelings, G., Pilate, G., 2012. Plant fiber formation: state of the art, recent and expected progress, and open questions. Crit. Rev. Plant. Sci. 31, 201–228. https://doi.org/10.1080/07352689.2011.616096.

Gorshkova, T., Morvan, C., 2006. Secondary cell-wall assembly in flax phloem fibres: role of galactans. Planta 223, 149–158. https://doi.org/10.1007/s00425-005-0118-7.

Gorshkova, T.A., Sal'nikov, V.V., Chemikosova, S.B., Ageeva, M.V., Pavlencheva, N.V., van Dam, J.E.G., 2003. The snap point: a transition point in Linum usitatissimum bast fiber development. Ind. Crops Prod. 18, 213–221. https://doi.org/10.1016/S0926-6690(03)00043-8.

Goubet, F., Bourlard, T., Girault, R., Alexandre, C., Vandevelde, M.-C., Morvan, C., 1995. Structural features of galactans from flax fibres. Carbohydr. Polym. 27, 221–227. https://doi.org/10.1016/0144-8617(95)00063-D.

Goudenhooft, C., Siniscalco, D., Arnould, O., Bourmaud, A., Sire, O., Gorshkova, T., Baley, C., 2018. Investigation of the mechanical properties of flax cell walls during plant development: the relation between performance and cell wall structure. Fibers 6, 6. https://doi.org/10.3390/fib6010006.

Hernandez, A., Westerhuis, Wim, van Dam, J.E.G., 2007. Microscopic study on hemp bast fibre formation. J. Nat. Fibers 3, 1–12. https://doi.org/10.1300/J395v03n04_01.

Hu, W., Ton-That, M.-T., Perrin-Sarazin, F., Denault, J., 2010. An improved method for single fiber tensile test of natural fibers. Polym. Eng. Sci. 50, 819–825. https://doi.org/10.1002/pen.21593.

Islam, M.S., Pickering, K.L., Foreman, N.J., 2011. Influence of alkali fiber treatment and fiber processing on the mechanical properties of hemp/epoxy composites. J. Appl. Polym. Sci. 119, 3696–3707. https://doi.org/10.1002/app.31335.

Kim, E.-S., Choi, W., Park, S.-H., 2021. The thickening and modification of the galactan-enriched layer during primary phloem fibre development in Cannabis sativa. AoB PLANTS 13 plab044. https://doi.org/10.1093/aobpla/plab044.

Kroon-Batenburg, L., Kroon, J., Northolt, M., 1986. Chain modulus and intramolecular hydrogen bonding in native and regenerated cellulose fibers. Polym. Commun.

Lefeuvre, A., Duigou, A.L., Bourmaud, A., Kervoelen, A., Morvan, C., Baley, C., 2015. Analysis of the role of the main constitutive polysaccharides in the flax fibre mechanical behaviour. Ind. Crops Prod. 76, 1039–1048. https://doi.org/10.1016/j.indcrop.2015.07.062.

Liu, M., Fernando, D., Daniel, G., Madsen, B., Meyer, A.S., Ale, M.T., heresen, A., 2015. Effect of harvest time and field retting duration on the chemical composition, morphology and mechanical properties of hemp fibers. Ind. Crops Prod. 69, 29–39. https://doi.org/10.1016/j.indcrop.2015.02.010.

Marrot, L., Lefeuvre, A., Pontoire, B., Bourmaud, A., Baley, C., 2013. Analysis of the hemp fiber mechanical properties and their scattering (Fedora 17). Ind. Crops Prod. 51, 317–327. https://doi.org/10.1016/j.indcrop.2013.09.026.

Mathel, V., Aziz, S., Guo, X., Bertling, K., Rakić, A.D., Heitzmann, M.T., Vandi, L.-J., 2025. Wood/PHAs biocomposites with mechanical properties comparable to conventional plastics: Model-based prediction and experimental validation. Compos. Part A Appl. Sci. Manuf. 194, 108916. https://doi.org/10.1016/j.compositesa.2025.108916.

Mediavilla, V., Leupin, M., Keller, A., 2001. Influence of the growth stage of industrial hemp on the yield formation in relation to certain fibre quality traits. Ind. Crops Prod. 13, 49–56. https://doi.org/10.1016/S0926-6690(00)00052-2.

Melelli, A., Arnould, O., Beaugrand, J., Bourmaud, A., 2020. The middle lamella of plant fibers used as composite reinforcement: investigation by atomic force microscopy. Molecules 25, 632. https://doi.org/10.3390/molecules25030632.

Meng, Y., Wang, S., Cai, Z., Young, T.M., Et, A., 2012. A novel sample preparation method to avoid influence of embedding medium during nano-indentation. Appl. Phys. A. https://doi.org/10.1007/s00339-012-7123-z.

Müssig, J., Amaducci, S., Bourmaud, A., Beaugrand, J., Shah, D.U., 2020. Transdisciplinary top-down review of hemp fibre composites: from an advanced product design to crop variety selection. Compos. Part. C Open. Access. 2, 100010. https://doi.org/10.1016/j.jcomc.2020.100010.

Müssig, J., Beaugrand, J., 2025. Decortication and separation of wet or dry hemp stems - What difference does it make? Ind. Crops Prod. 223, 119965. https://doi.org/10.1016/j.indcrop.2024.119965.

Nuez, L., Gautreau, M., Mayer-Laigle, C., D'Arras, P., Guillon, F., Bourmaud, A., Baley, C., Beaugrand, J., 2020. Determinant morphological features of flax plant products and their contribution in injection moulded composite reinforcement. Compos. Part. C Open. Access. 3, 100054. https://doi.org/10.1016/j.jcomc.2020.100054.

Pinsard, L., Revol, N., Pomikal, H., De Luycker, E., Ouagne, P., 2023. Production of long hemp fibers using the flax value chain. Fibers 11, 38. https://doi.org/10.3390/fib11050038.

Placet, V., 2009. Characterization of the thermo-mechanical behaviour of Hemp fibres intended for the manufacturing of high performance composites. Composites Part A: Applied Science and Manufacturing, Special Issue: 15th French National Conference on Composites - JNC15 40, 1111–1118. https://doi.org/10.1016/j.compositesa.2009.04.031.

Placet, V., Day, A., Beaugrand, J., 2017. The influence of unintended field retting on the physicochemical and mechanical properties of industrial hemp bast fibres. J. Mater. Sci. 52, 5759–5777. https://doi.org/10.1007/s10853-017-0811-5.

Salmén, L., 2004. Micromechanical understanding of the cell-wall structure. Comptes Rendus Biol. 327, 873–880. https://doi.org/10.1016/j.crvi.2004.03.010.

Sawpan, M.A., Pickering, K.L., Fernyhough, A., 2011. Effect of various chemical treatments on the fibre structure and tensile properties of industrial hemp fibres. Composites Part A Applied Science Manufacturing 42, 888–895. https://doi.org/10.1016/j.compositesa.2011.03.008.

Schäfer, T., Honermeier, B., 2006. Effect of sowing date and plant density on the cell morphology of hemp (Cannabis sativa L.). Ind. Crops Prod. 23, 88–98. https://doi.org/10.1016/j.indcrop.2005.04.003.

Small, E., 2015. Evolution and Classification of Cannabis sativa (Marijuana, Hemp) in Relation to Human Utilization. Bot. Rev. 81, 189–294. https://doi.org/10.1007/s12229-015-9157-3.

Snegireva, A., Chernova, T., Ageeva, M., Lev-Yadun, S., Gorshkova, T., 2015. Intrusive growth of primary and secondary phloem fibres in hemp stem determines fibre-bundle formation and structure. AoB PLANTS 7 plv061. https://doi.org/10.1093/aobpla/plv061.

Stamboulis, A., Baillie, C.A., Peijs, T., 2001. Effects of environmental conditions on mechanical and physical properties of flax fibers. Compos. Part A Appl. Sci. Manuf. 32, 1105–1115. https://doi.org/10.1016/S1359-835X(01)00032-X.

Wiley, J.H., Atalla, R.H., 1987. Band assignments in the raman spectra of celluloses. Carbohydrate Research 160, 113–129. https://doi.org/10.1016/0008-6215(87)80306-3.

Ying, R., Saulnier, L., Rondeau-Mouro, C., 2011. Films of arabinoxylans and β-glucans extracted from cereal grains: Molecular motions by TD NMR. Carbohydr. Polym. 86, 812–822. https://doi.org/10.1016/j.carbpol.2011.05.033.

Ying, R., Saulnier, L., Bouchet, B., Barron, C., Ji, S., Rondeau-Mouro, C., 2015. Multiscale characterization of arabinoxylan and β-glucan composite films. Carbohydr. Polym. 122, 248–254. https://doi.org/10.1016/j.carbpol.2015.01.014.

Yuan, Z., Nag, R., Cummins, E., 2022. Human health concerns regarding microplastics in the aquatic environment - From marine to food systems. Sci. Total. Environ. 823, 153730. https://doi.org/10.1016/j.scitotenv.2022.153730.

Zafeiropoulos, N.E., Baillie, C.A., 2007. A study of the effect of surface treatments on the tensile strength of flax fibres: Part II. Application of Weibull statistics. Compos. Part A Appl. Sci. Manuf. 38, 629–638. https://doi.org/10.1016/j.compositesa.2006.02.005.

Zamil, M., Geitmann, A., 2017. The middle lamella-more than a glue. Phys. Biol. 14. https://doi.org/10.1088/1478-3975/aa5ba5.